

# Influence of different interface materials and openings in infill of reinforced concrete infilled frames

Vishali Mugunth Kumar<sup>1</sup>, Satyanarayanan Kachabeswara Srinivasan<sup>1</sup>, Thirumurugan Varatharajan<sup>1</sup> and Prakash Murugan<sup>1</sup>

<sup>1</sup> SRM Institute of Science and Technology, Faculty of Engineering and Technology, Department of Civil Engineering, SRM Nagar, Kattankulathur, 603-203, Tamil Nadu, India

**Corresponding author:**

Vishali Mugunth Kumar  
[vm4814@srmist.edu.in](mailto:vm4814@srmist.edu.in)

**Received:**

September 26, 2022

**Accepted:**

December 23, 2022

**Published:**

March 28, 2023

**Citation:**

Vishali, M.; Satyanarayanan, K. S.; Thirumurugan, V.; and Prakash, M. (2023). Influence of different interface materials and openings in infill of reinforced concrete infilled frames. *Advances in Civil and Architectural Engineering*. Vol. 14, Issue No. 26. pp.54-79  
<https://doi.org/10.13167/2023.26.5>

**ADVANCES IN CIVIL AND ARCHITECTURAL ENGINEERING (ISSN 2975-3848)**

Faculty of Civil Engineering and Architecture Osijek  
Josip Juraj Strossmayer University of Osijek  
Vladimira Preloga 3  
31000 Osijek  
CROATIA



**Abstract:**

This study analytically investigates the behaviour of trapezoidal infilled frames (TIFs) with brick masonry infills having openings and various interface materials between the brick panel and reinforced concrete frame. Single-storey single-bay frame specimens are analysed under in-plane static loading. For this investigation, the optimum angle of the column inclination for the trapezoidal frame must be determined in terms of maximum lateral stiffness. The optimum angle must be further analysed and compared with rectangular bare and infilled frames, with various materials of the interface. This infilled frame is extended to analyse the openings in the infill further. To study the effects of openings in infilled panels, TIFs with different sizes and positions of window openings are analysed and compared with the rectangular frame. This study further analyses three different combinations of interfaces and determines the intermediate stiffness of the frame combination. The main focus of this investigation is to reduce the high rigidity of the TIF leading to high base shear. It is found that, the infilled frame is stiffer than the bare frame, and the cement mortar interface is stiffer than the lead-cork interface. This research uses ABAQUS software, a finite element analysis program, for expanding the observational analysis.

**Keywords:**

trapezoidal frame; rectangular frame; RC frame; masonry infill; interface; opening; lateral stiffness; static loading; finite element analysis

## 1 Introduction

High-rise buildings have become increasingly essential. This is because of high population density problems and the scarcity of land for development. These buildings require a special structural system to sustain lateral loads, such as wind and seismic loads. One of the most common lateral load-resisting structures is an infilled frame. In developing countries, such as Argentina, Portugal, and India, some 30-storey buildings were built using this infilled frame as a lateral load resisting system without the use of shear walls [1]. Figure 1 shows some of the reinforced concrete (RC) infilled frame structures in Argentina, Portugal, Venezuela, and India.

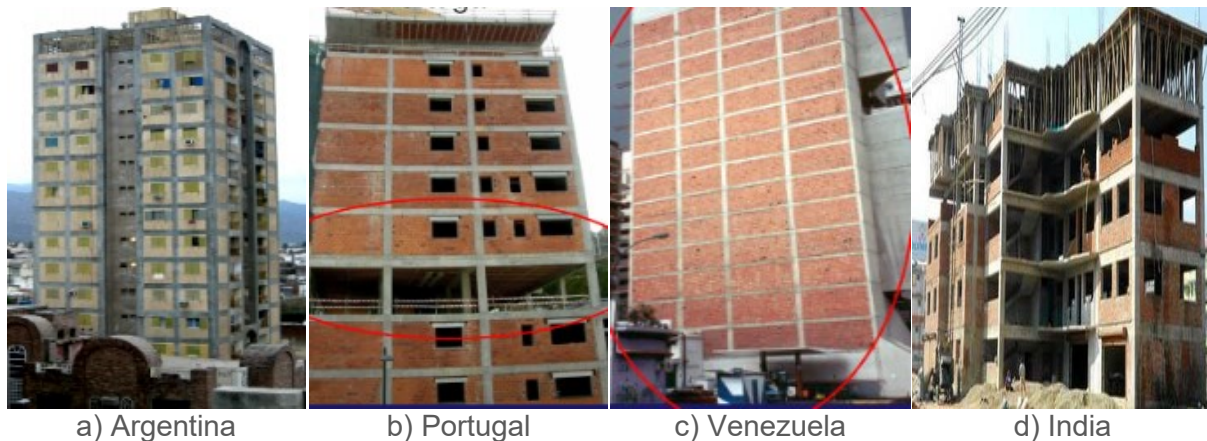


**Figure 1. RC infilled frame structures [2,3]**

Infilled frames are beam and column frameworks with masonry walls infilling a few bays of the frame that may or may not be mechanically attached. Masonry RC infilled frames are widely used and regularly utilised in various structural systems, as shown in Figure 2. Among construction materials, brick masonry is commonly utilised as an infill because of its popularity and obtainability. It is also recognised as a traditional building and construction material. These masonry infilled walls are frequently observed in exterior walls, interior walls, and walls around stairs [4]. A frame with an infill has significant lateral stiffness, strength, ductility, energy dissipation capacity, and rigidity compared with a bare frame [5]. This is economically significant for tall buildings that are subjected to strong lateral loads.

An experimental investigation of the macro-modelling approach with loading perpendicular to the surface (i.e., out-of-plane loading) was performed. A study of the behaviour of two types of brick masonry infilled walls and their calibration was also performed for a numerical model based on experimental results [6]. Karayannis experimentally and analytically investigated the seismic response of an RC frame under the influence of a solid masonry infill [7]. Jurko studied single-bay RC frames with various masonry infill materials and found that composite frame wall structures had higher stiffness, damping, and initial strength than bare frame structures [8]. Chao suggested two unique infilled pre-fabricated damping wall panels for semi-rigid steel frames and conducted an experiment to investigate their seismic reactions [9]. The behaviour and effects of infilled walls have been widely recognised by multiple studies over the past few decades. Calvi conducted extensive research on infilled frames [10]. In [11] and subsequently described the behaviour of infilled frames under lateral loads [12].

Most recent studies have investigated whether properly designed infills can improve the earthquake resistance of frame structures. These structures have shown excellent performance under few moderate earthquakes in seismic regions even when the buildings have not been properly designed and detailed to resist earthquake forces. When an earthquake occurs, the infill can strengthen the upper storey of the structure and form a soft first storey; however, this is unacceptable from the perspective of an earthquake-resistant

building [13]. The following were investigated based on the effects of infilled frames on structures under seismic action [14-20].

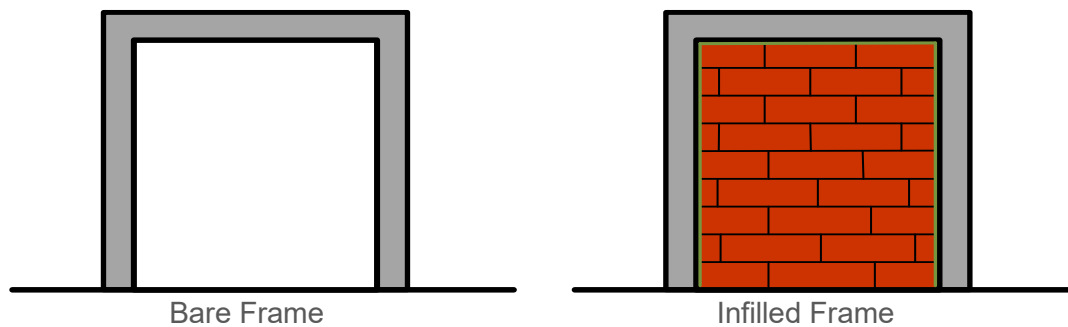


**Figure 2. Infilled frame with and without brick masonry**

Some parameters affect the strength, deformation, and stiffness of infills. These factors include openings in the infill, lateral loads, infills, and interface materials [21]. The interface is surrounded by a frame and infill, as shown in Figure 3. The ductility of the structure improves when the load transfer to the interface materials occurs midway between the frame and infilled panel. The main aim of providing a gap filling is to improve acoustic performance and heat resistance under seclusion [22]. Diagonal strut bracing action was verified to be provided by the stiffness of the infill [23], thus improving the structural system. The results of the study are affected by the model adopted, type of analysis implemented [24], condition of the interface, and construction details affecting the infilled frame behaviour [25].

As reported in [26], two-bay three-storey bare and infilled RC frames with a scale ratio of 1:6 was experimentally investigated under static cyclic loading; three different types of interfaces were used in the middle of the infill and frame. Senthil [27] investigated the behaviour of a two-dimensional (2D) RC infilled frame with different interface thicknesses subjected to lateral loads. The behaviour of RC infilled frames with various interface materials, such as cement mortar, lead, cork, and pneumatic air medium, has been investigated [28]. Zeeshan [29] investigated the use of polyethylene foam as an interface in RC infilled frames for the seismic isolation of masonry infills.

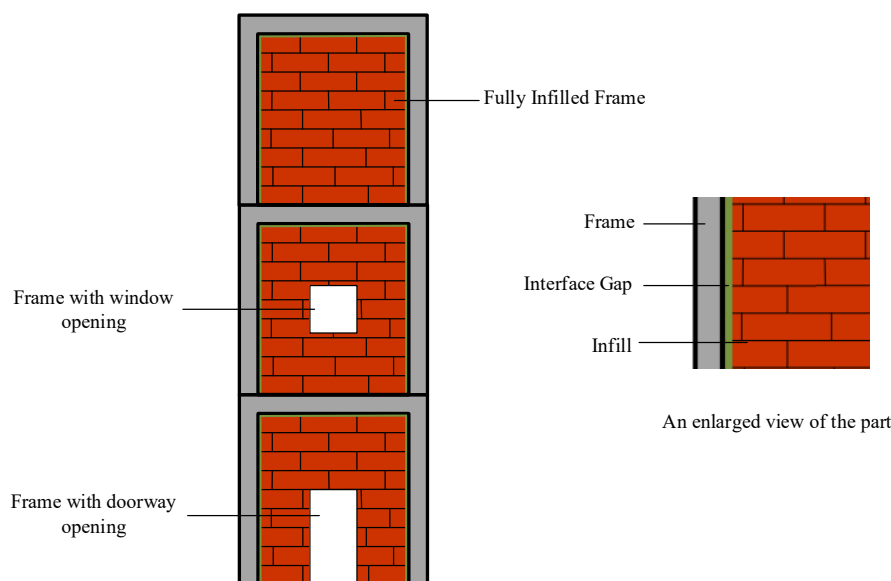


**Figure 3. Typical infilled frames**

Infilled panels with openings are best viewed as a collection of subcomponents of appropriate materials. Furthermore, for functional reasons, openings (such as windows and doors) play an important role in infilled frames. These openings in the infill modify panel behaviour, which is influenced by numerous factors, such as the size and location of the openings. The two most predominant forms of openings are doors and windows [30]. The behaviour of frames is influenced by the opening of infilled walls (doors and windows). The effect of openings on the resultant lateral stiffness and strength of such frames has gained considerable attention in recent studies. During the action of lateral loads, the infilled panel with openings generally fails near the opening owing to stress concentration [31]. In previous studies, infilled panels with openings were found to provide significant lateral stiffness and strength to a frame. In a specific investigation, frames with an opening area exceeding 50 % with respect to the total infilled area tend to behave as bare frames [32].

One study used a non-contact technique to measure strain and deformation in an experimental investigation of the out-of-plane response of RC frames with masonry infilled walls; the frames were with and without openings (i.e., doors and windows) [33]. In [34], the development of a multi-strut model for masonry infilled frames with various opening configurations (i.e., different sizes and positions) was reported; the overall force displacement for these configurations was also simulated. Mallick [35] experimentally studied the impact of various positions of openings on infilled frames with lateral stiffness as well as on infilled frames with and without shear connections. In [36], the experimental testing of five RC infilled frames with various opening proportions was reported. Based on the findings, a foundation was laid for improving the performance of an infilled frame with openings, thus reducing the danger of progressive collapse.

Liborio extensively studied computational experimental campaigns based on finite element (FE) models by reducing the out-of-plane stiffness and strength owing to in-plane damage [37]. Minas built an analytical model of a steel moment-resisting frame with brick masonry infills for estimating the initial lateral stiffness [38]. Liborio summarised the findings of an actual case study on the seismic performance of an RC school structure. The model was evaluated by concentric equivalent struts to model the infill. The additional shear introduced to the column led to the discovery of a correlation based on numerical observation [39]. Asteris investigated a number of 14-storey RC infilled frame buildings with a fundamental period of vibration using an FE macro-model and eigenvalue analysis [40]. An in-depth analytical investigation of various parameters affecting the fundamental period of the RC structure was also conducted [41].



**Figure 4. Buildings with trapezoidal frame [42–44]**

Joao performed complete research based on four primary vectors affecting seismically vulnerable RC structures. These factors include international code guidelines and insight gained from the observation of seismic behaviour, experiments, and numerical modelling. The order in which they should be used (divided into macro-modelling and micro-modelling) was investigated [44].

According to available reports in literature, only rectangular-shaped and square-shaped infilled frames have been investigated to a considerable extent. However, trapezoidal infilled frames

(TIFs), which provide more lateral stiffness than normal rectangular and square-shaped infilled frames, require further study. Some examples of trapezoidal buildings are shown in Figure 4. The foregoing studies demonstrate the importance of the configuration of a structure because high-rise structures with typical shapes, such as square-type and rectangular-type buildings, are unable to withstand lateral loads. A new configuration, known as trapezoidal frames, has been adopted to improve the lateral stiffness of such buildings.

To fill this research gap, a 2D RC trapezoidal frame configuration was analysed, and the behaviour of the structure was investigated. The structure was modelled and analysed using the ABAQUS FE analysis (FEA) software package. Because columns are the most significant part of a structure, an optimum angle analysis was performed. A fixed optimum angle was analysed using an infilled frame with different interface materials under static lateral loads. Various sizes and positions of openings in the infilled panel were investigated in the TIF using various interface materials. In this study, the bare frame and cork interface materials are also known as bare frames and soft interface materials, respectively.

The in-plane lateral behaviour of a trapezoidal frame with an infill has become significant because of the increasing use of inclined columns to satisfy the demand for longer spacing among columns. The use of inclined columns from the base has also become popular, resulting in the formation of trapezoidal frames. Because these frames may have higher stiffness than rectangular or square frames, they attract greater base shear. Infilling these frames is expected to further increase the magnitude of this base shear to a higher level. Hence, gaining more knowledge in this area is relevant, especially with the aim of controlling the increase in base shear by introducing soft materials to the interface gap between the frame and infill.

A number of studies have been performed on infilled frames with straight columns known as rectangular or square frames. However, studies on infilled frames with inclined columns, known as TIFs, are limited. The investigation of the influence of different interface materials and infill openings on trapezoidal frames is limited. Therefore, comprehensive studies related to different interface materials and openings in infilled panels must be conducted.

## 2 Properties of interface materials

The material properties of a single-bay single-storey frame with a column size of 400 × 300 mm, beam size of 300 × 300 mm, and storey height of 3500 mm with different interface materials are described below.

The properties of interface materials are presented in the following sections. In an analytical investigation, an element surrounded by an infilled panel and RC frame is termed as interface medium. Different interface materials, namely cement mortar, lead, and cork are investigated. They are 10 mm thick and the width corresponds to that of the masonry. In construction practice, soft materials with viscoelastic properties are commonly used at the interface to avoid vertical cracking of the infilled functional wall owing to the vertical load transfer from the frame because of the deformation caused by the load, thermal effects, or both.

In practice, these materials are cork, rubberised corks, and lead. Lead and cork are used in this study.

### 2.1 Cement mortar interface

Cement mortar is used as the interface between the frame and infill. It is the same cement mortar used in laying brick masonry works. Experimental results on cement mortar (Figure 5) show that the mortar's compressive strength and elastic modulus are 2,78 and 27386 N/mm<sup>2</sup>, respectively.

The density and Poisson's ratio of cement mortar selected from literature are 18,02 kN/m<sup>3</sup> and 0,15; respectively [23].



Figure 5. Cement mortar specimen

## 2.2 Lead interface

A 10-mm-thick non-structural lead material was used as interface material to study its effect on and behaviour in the infilled frame system. The basic stress–strain behaviour of the lead sheet was estimated by tensile test experiments.

The elastic modulus of lead obtained from literature was  $8000 \text{ N/mm}^2$  [45, 46]. The selected Poisson's ratio and density were 0,447 and  $111,210 \text{ kN/m}^3$ , respectively.

The stress–strain graph of the lead sheet is shown in Figure 6.

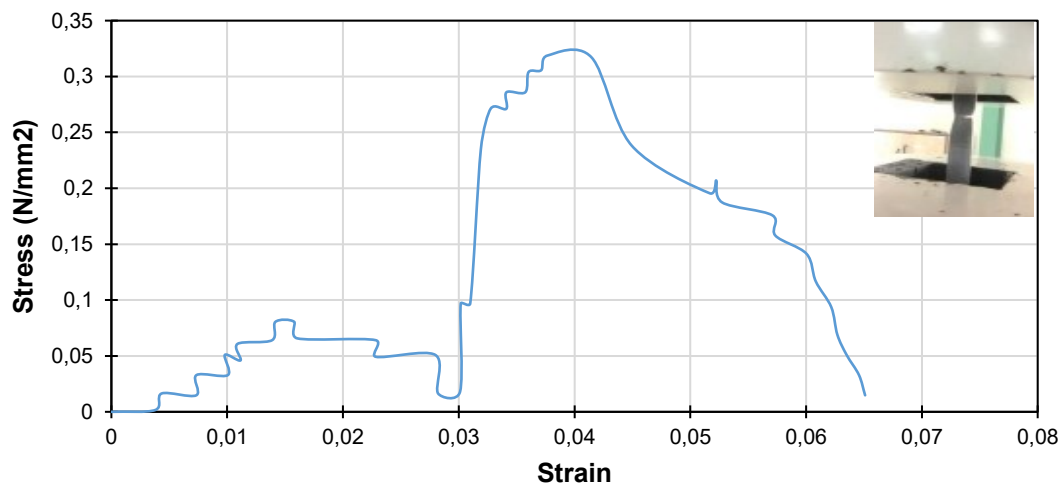


Figure 6. Stress–strain diagram of lead sheet

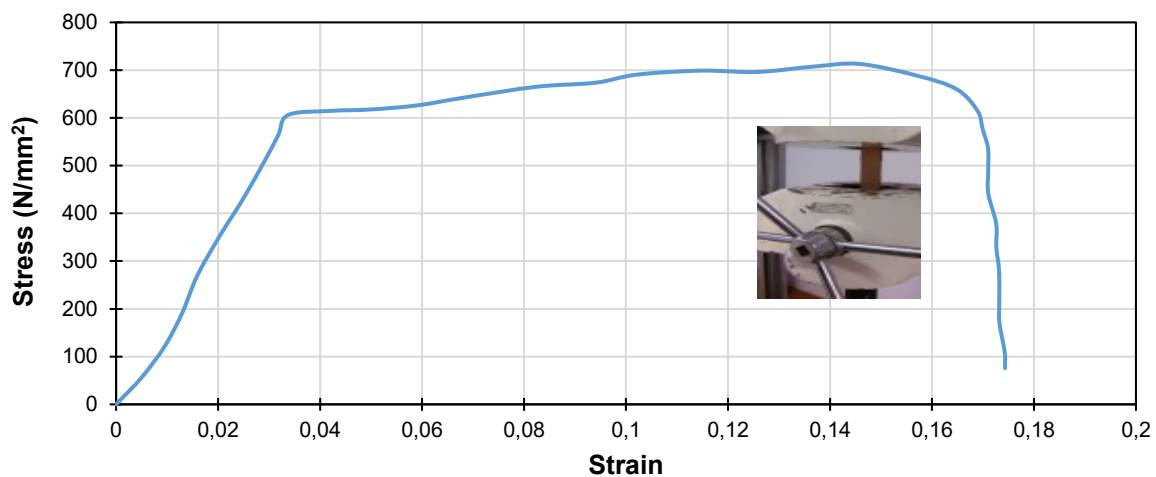
Tensile test was performed on the lead sheet material using a TUE-C-1000 machine. The test data are listed in Table 1.

**Table 1. Tensile test results of lead sheet**

Input Data		Output Data	
sample shape	Flat	load at yield	0,16 kN
sample type	Lead Sheet	elongation at yield	4,880 mm
sample description	1	yield stress	0,254 N/mm <sup>2</sup>
sample width	210 mm	load at peak	0,200 kN
sample thickness	10 mm	elongation at peak	6,170 mm
gauge length for % elongation	150 mm	tensile strength	0,317 N/mm <sup>2</sup>
pre-load value	0 kN	load at break	0,010 kN
max. load	1000 kN	elongation at break	9,760 mm
max. elongation	200 mm	% reduction area	52,38
specimen C.S. area	630 mm <sup>2</sup>	% elongation	6,67

### 2.3 Cork interface

A 10-mm-thick non-structural cork material was used as the interface material between the frame and infill. The basic stress–strain behaviour of the cork sheet was evaluated by tensile test. The elastic modulus of cork obtained from [47] was 12,6 N/mm<sup>2</sup>. The selected Poisson's ratio and density are 0,097 and 1,765 kN/m<sup>3</sup>, respectively. Figure 7 shows the stress–strain curve of the cork sheet.

**Figure 7. Stress–strain diagram of cork sheet**

Tensile tests were performed on the cork sheet material using the TUE-C-1000 machine. Table 2 lists the output data.

**Table 2. Tensile test results of cork sheets**

Input Data		Output Data	
sample shape	Solid Flat	load at yield	59,35 kN
sample type	Cork Sheet	elongation at yield	6,150 mm
sample thickness	10 mm	yield stress	524,77 N/mm <sup>2</sup>
sample diameter	12 mm	load at peak	76,690 kN
gauge length for % elongation	200 mm	elongation at peak	26,010 mm
pre-load value	0 kN	tensile strength	678,089 N/mm <sup>2</sup>
final SP diameter	8,7 mm	load at break	55,830 kN
final gauge length	223 mm	elongation at break	32,740 mm
final area	59,45 mm <sup>2</sup>	% reduction area	47,44
specimen cross-sectional area	113,1 mm <sup>2</sup>	% elongation	11,50

The mechanical properties and compressive strengths of the interface materials are based on Poisson's ratio and density values assumed based on literature, as summarised in Table 3.

**Table 3. Mechanical characteristics of materials used**

Material name	Specifications	Elastic modulus (N/mm <sup>2</sup> )	Poisson's ratio	Density (kN/m <sup>3</sup> )
concrete (m30)*	M30 grade; Average compression strength of 35,20 N/mm <sup>2</sup>	$5000\sqrt{f_{ck}} = 27\ 386$	0,23	23,53
reinforcement*	Fe415	200 000	0,30	76,98
infilled (brick masonry) *	Class II brick masonry; strength: 4,175 N/mm <sup>2</sup>	1020	0,22	13,27
interface (cement mortar)**	Thickness: 10 mm; strength: 2,78 N/mm <sup>2</sup>	27386	0,15	18,02
interface (lead)***	10-mm-thick sheet	8000	0,447	111,210
interface (cork)****	10-mm-thick sheet	12,6	0,097	1,765

Notes: \* Muthukumar (2019) [26], \*\*Achyutha et al. (1994) [45], \*\*\*Riddington and Sahota (2003) [46], \*\*\*\* Silva et al. (2005) [47].

### 3 Analytical investigation

#### 3.1 Modelling and analysis

The single-bay single-storey 2D RC trapezoidal frame was modelled as a solid element using the FEA software ABAQUS. The beam and column frame members were designed as line elements, and the interface and infill were designed as plane stress elements. Figure 8 shows the frame members as beam elements with three degrees of freedom per node. Figure 9 shows the infill as a four-node plane stress element with two degrees of freedom per node and homogeneous masonry characteristics. In the case of an infilled frame, the interface linking the frame to the infill was also modelled using four-node plane stress components with two degrees of freedom per node and different interface characteristics, as shown in Figure 9.

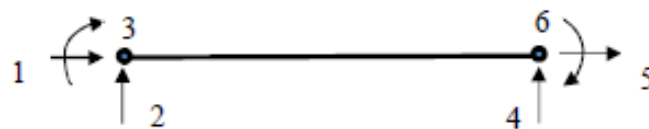


**Figure 8. Beam element for frame member**

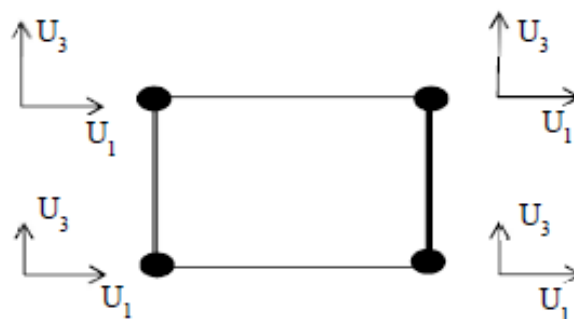


**Figure 9. Four-node plane stress elements used in infill**



**Figure 10. Test of normal and inclined bed joints**

Modelling was based on homogenous isotropic properties. However, a part of the investigation (not shown in this paper) includes the effects of principal stress orientation on the bed joint (Figure 10) and the corresponding mechanical properties for the analysis; the results do not differ significantly. The support conditions for the frames are fixed. M30-grade concrete and Fe415-grade steel reinforcement were used in all the cases. The same material characteristics, namely density, Young's modulus, and Poisson's ratio, are also adopted in all cases, as listed in Table 3. The dimensions of members and details of reinforcement are listed in Table 4

**Table 4. Dimensions and reinforcement of 2D trapezoidal RC frame**

Member	Dimensions (mm)	Clear Cover (mm)	Main Steel Bars	Stirrups/Ties
beam	300 × 300	30	4-12-mm diameter bars	8-mm-diameter bars @ 150 mm C/C
column	400 × 300	40	4-16-mm-diameter and 2 12-mm-diameter bars	8-mm-diameter @ 150 mm C/C

### 3.2 Meshing and discretisation

A convergence investigation of the infill element was performed in developing an FE model (FEM) of the infilled frame to attain constant stiffness for the solid element. Discretisation is the process of converting an object-based model's material domain into an analytical model that is appropriate for analysis.

In approximating the FE analysis, the element is discretised to obtain results that are sufficiently close to convergence. A mesh convergence investigation was performed on the infill with element mesh size ranging from 5 × 5 to 50 × 50. A load of 1 kN was applied to the infill for analysis. Mesh sensitivity was investigated in terms of frame displacement, strain in the infill, and monotonic convergence in terms of displacement. As a result, only the

displacement was considered in the mesh sensitivity analyses. The frame displacement was constant up to a mesh size of  $50 \times 50$ . Based on the mesh convergence investigation, the mesh size used in all the elements throughout the analytical work was  $50 \times 50$  mm. Figure 11 depicts the evolution of the curve into an asymptote, displaying linear variation once the element size is  $50 \times 50$  or larger. The rest of the analysis was performed using the  $50 \times 50$  grid discretisation pattern.

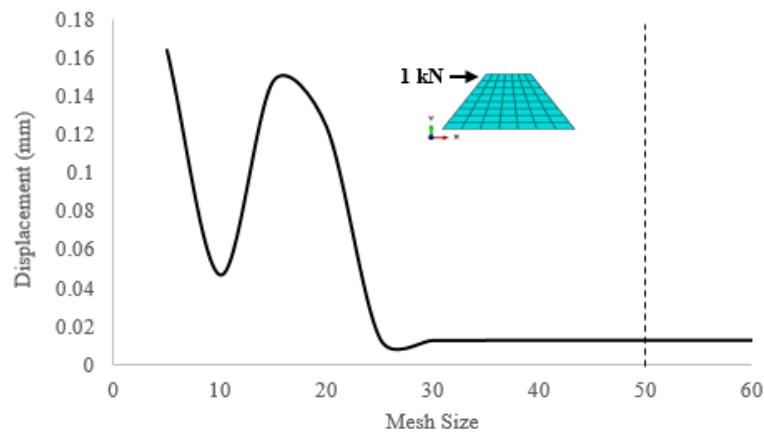


Figure 11. Convergence study

### 3.3 Loading and Interaction

Loading is an important project module for interpreting outcomes. A 10-kN static monotonic lateral load was applied to the top left beam–column intersection. The interaction between the reinforcement (embedded region) and RC frame (host region) was designated as embedded interaction. A tie constraint with a discretisation method of surface-to-surface interaction was designed for the interface material and infilled wall.

## 4 Results and discussion

A linear FEA was performed for both configurations. Because studies on trapezoidal frames are limited, in this study the elastic behaviour is first investigated. By analysing the models under various situations and scenarios, the essential structural features, such as lateral stiffness, axial load, bending moment, and shear force, are evaluated.

### 4.1 Study of optimum angle for trapezoidal frame configuration through FEM analysis

Different angles were considered to examine the optimum angle for the trapezoidal frame configuration under static loading. The frames were treated as both bare and infilled frames. For each configuration, i.e., (a) trapezoidal bare frame (TBF) and (b) TIF with brick masonry, 10 angles were considered. Table 5 lists the specifications of the prototype of the two frame configurations considered for the analysis.

Table 5. Details of 2D trapezoidal frame

Sl. No.	Frame details		Dimensions (mm)			Description of Materials	
			Members	Top Width	Storey Height	Frame	Infill
1	bare frame	BF	column: 400 × 300 beam: 300 × 300	3000	3500	Fe 415-grade Steel; M30-grade concrete	Compressive strength of brick masonry = 1,54 N/mm <sup>2</sup> ; wall thickness = 230 mm
2	infilled frame	IF					

### 4.2 Lateral stiffness

Lateral stiffness was calculated based on the applied lateral load and the resulting horizontal displacement with respect to the frame. The linear analysis indicates that the lateral stiffness of an RC frame with an infilled panel is greater than that of a bare frame because the infilled panel resists the lateral load [12]. The stiffness  $K$  in each configuration is calculated using Eq. (1):

$$K = \frac{F}{\Delta_x} \tag{1}$$

Where:

$F$  denotes load applied to the member, and  
 $\Delta_x$  denotes displacement of the member in the X direction.

Figure 12 shows that the stiffness of the bare frame is higher when the column’s angle of inclination exceeds 70°. The data value fluctuation is depicted by a polynomial curve.

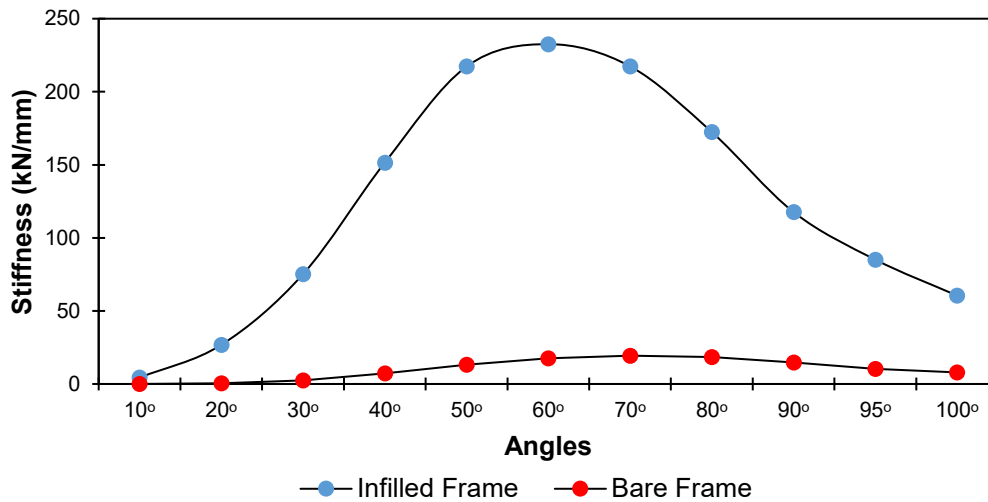


**Figure 12. Optimisation of column inclination for bare frame and infilled frames**

A new parameter is introduced to the trendline. An order value can be specified to determine the maximum number of variations or bends of the line. When data fluctuate, a polynomial trendline, i.e., a curve, is employed. With the polynomial equation in the trendline option, Eq. (2) is used:

$$K = -0,0052\theta^2 + 0,7573\theta - 11,243; \frac{dK}{d\theta} = -2 \cdot (0,0052) \cdot \theta + 0,7573 \rightarrow \theta = 72,81^\circ \tag{2}$$

Because the analysis is optimised with the infilled frame at various angles under the influence of static lateral loading with respect to lateral stiffness, the infilled frame has a 10-mm-thick cement mortar interface in all cases. Figure 12 also shows the optimisation of the column inclination for the infilled frame. Similarly, using the polynomial equation for optimising the column inclination of the infilled frame, Eq. (3) is derived:

$$K = -0,0959\theta^2 + 11,633\theta - 142,6; \frac{dK}{d\theta} = -2 \cdot (0,0959) \cdot \theta + 11,633 \rightarrow \theta = 60,65^\circ \tag{3}$$

The foregoing analysis clearly shows that a 60° angle is optimal for the column inclination, as indicated by the maximum stiffness of the infilled frame. Therefore, the optimum column inclination angle of the TIF is 60°.

### 4.3 Comparative study

An analytical study was conducted using two configurations. A trapezoidal frame configuration with an optimum angle was found in the previous analysis. The analytical models were designed using the limit state design method according to IS 456:2000 [52]. The dimensions and reinforcements for the 2D RC trapezoidal frame configuration were the same as those used in a previous study. The rectangular frame configuration is modelled and analysed with the indicated dimensions and reinforcement details listed in Table 6.

**Table 6. Details of 2D RC rectangular frame**

Description	Member size			Reinforcement details*	Material description
	Length C/C (mm)	Breadth (mm)	Depth (mm)		
Beam	3000	300	300	4-12-mm-diameter bars	M30-grade concrete and Fe415-grade steel
Column	3500	400	300	4-16-mm-diameter and 2 12-mm-diameter bars	

Note: \*8-mm stirrups @ 150 mm C/C.

Four types of frame configuration were used in this investigation. Their designations are listed in Table 7. The cross-sections of the trapezoidal and rectangular frames are shown in Figure 13.

**Table 7. Designation of frame configurations**

Frame Designation	Description
RBF	rectangular bare frame
RIF	rectangular infilled frame
TBF	trapezoidal bare frame
TIF	trapezoidal infilled frame

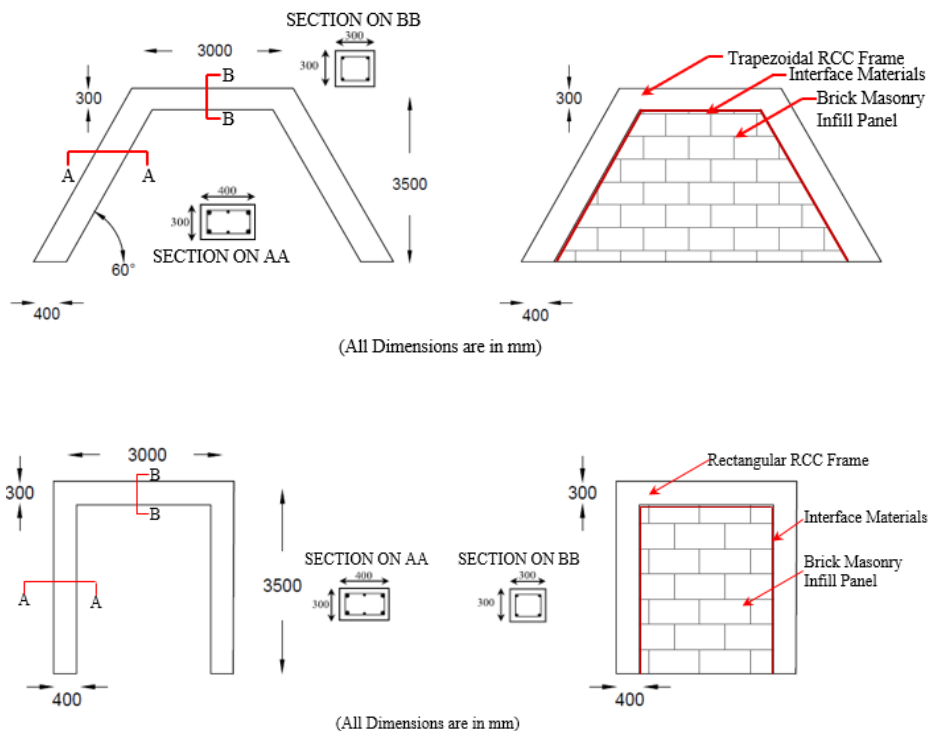


**Figure 13. Details of RC frame**

This section compares and discusses the findings of the linear FEM analysis conducted on four structural features: lateral stiffness, axial load, bending moment, and shear force.

#### 4.3.1 Lateral stiffness

Stiffness was evaluated by applying a lateral load horizontally to generate displacement along the x direction. A comparison of the stiffnesses is shown in Figure 14. Compared with the other three configurations, the TIF has the highest stiffness (289 kN/mm). In the bare frame, the lowest stiffness was found in the rectangular frame structure; the stiffness was 17 % lower than that of the trapezoidal frame structures. The rigidity of trapezoidal frame structures compared with that of rectangular frames increases by 50 % when an infilled frame is used.

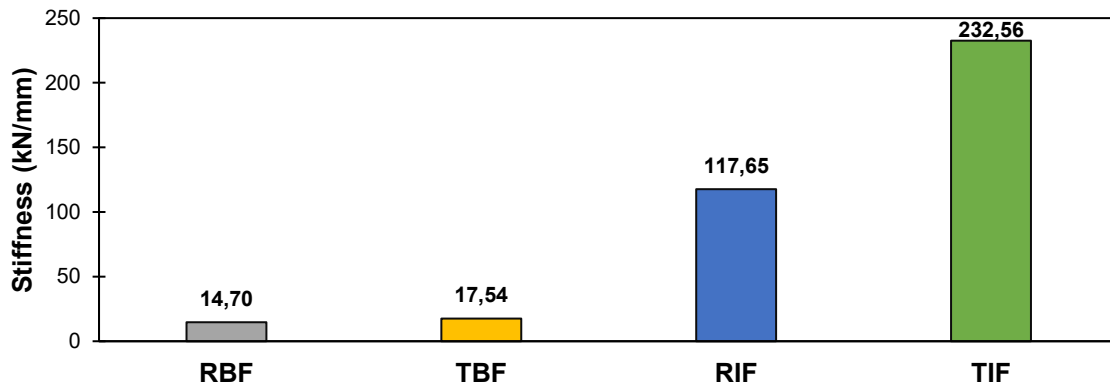


Figure 14. Comparison of stiffness

The stiffness of the trapezoidal frame configuration is higher than that of the rectangular frame configuration. This is because the column inclination at the 60° angle results in higher frame stiffness than a column inclination of 90°.

#### 4.3.2 Axial Load

A 10-kN static monotonic concentrated lateral load was applied to the top left beam–column junction. The maximum axial load was 10,91 kN in the RIF. The rectangular frame better absorbs the lateral load than the trapezoidal frame because its column inclined at 60° reacts as a rigid structure.

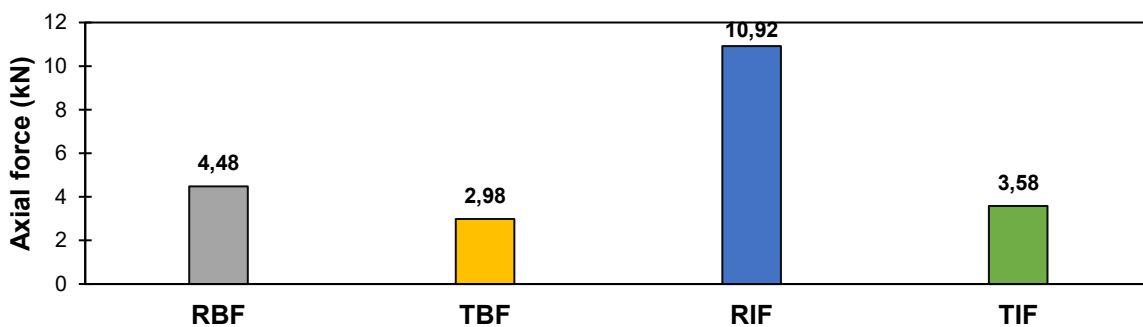
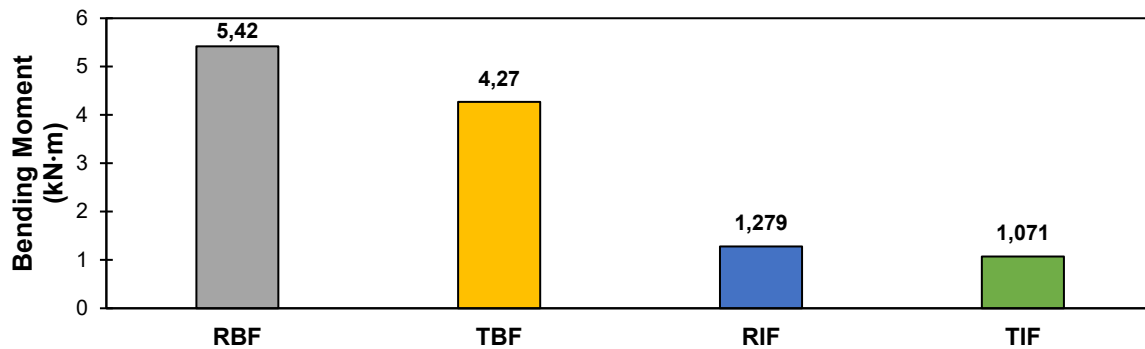


Figure 15. Comparison of axial force

The RBF sustains an axial load of 4,51 kN, which is 51 % higher than that borne by the TBF. As for the infilled frame, the axial load in the rectangular frame is 70 % higher than that in the trapezoidal frame (Figure 15).

### 4.3.3 Bending Moment

Structures, such as load-carrying frames and RC frames, can provide excellent earthquake protection when the beam–column intersection is perfectly constructed [48]. The moments at the beam–column junctions of the trapezoidal and rectangular frame configurations were obtained and compared. In both configurations, the bare frame had a higher bending moment than the infilled frame.



**Figure 16. Bending moment comparison**

Compared with the bare frame, additional strength and constraints are provided by the infilled panel to the infilled frames. The moment of the TBF is 4,27 kNm, which is 21 % less than that of the RBF. The bending moment of the TIF is 0,071 kNm, which is 74 % lower than that of the RIF. Figure 16 shows a graphical representation of the bending moment for all cases.

### 4.3.4 Shear force

The shear force at the beam–column intersection was also simulated. The linear analysis clearly shows that the shear force of the bare frame is greater than that of the infilled frames [49]. Figure 17 shows that the shear force of the infilled frame was lower than that of the bare frame.

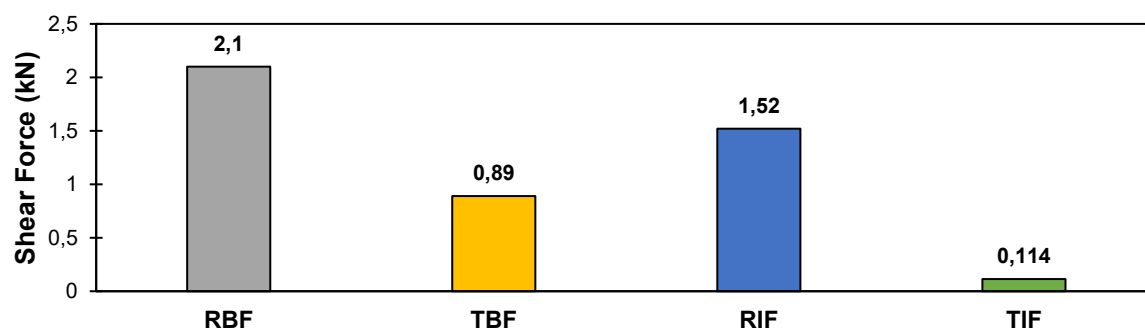


**Figure 17. Shear force comparison**

Among the four cases, the maximum shear force, 2,1 kN, occurs in the RBF. However, in the case of the infilled frame, the maximum shear force appears in the rectangular structures; the force is 90 % greater than that in the trapezoidal structures. In the case of the bare frame, the shear force of the trapezoidal frame configuration is 60 % lower than that of the rectangular frame structure. Validation is an important aspect of analytical studies.

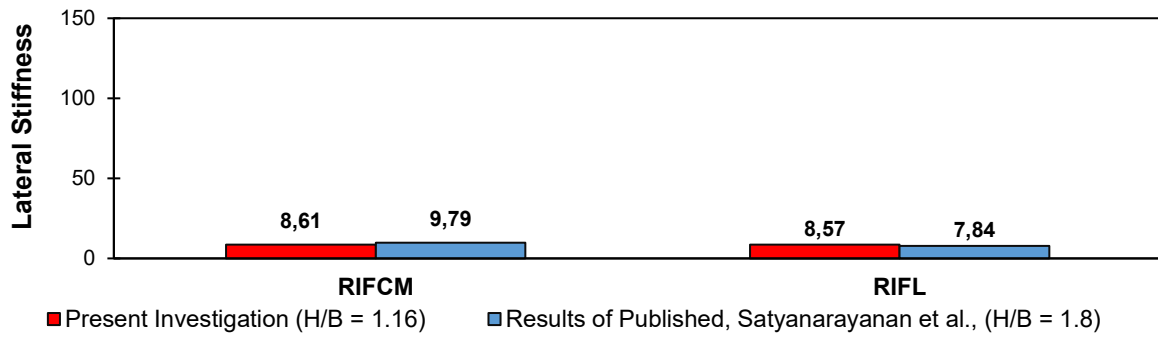


Figure 18. Validation study for rectangular frame

As shown in Figure 18, the RIF with different interface materials is verified and validated in a previous investigation [23].

4.4 Analytical study of elastic behaviour of TIF with different interface materials under static monotonic lateral load

Modelling and analysis were implemented using a FEA software package tool. A single-bay single-storey trapezoidal bare frame was initially modelled. Then, a single-bay single-storey trapezoidal RC infilled frame was also modelled and analysed. Tables 4 and 5 list the frame dimensions and reinforcement details. Two-node beam elements with two degrees of freedom were utilised to model the frame elements

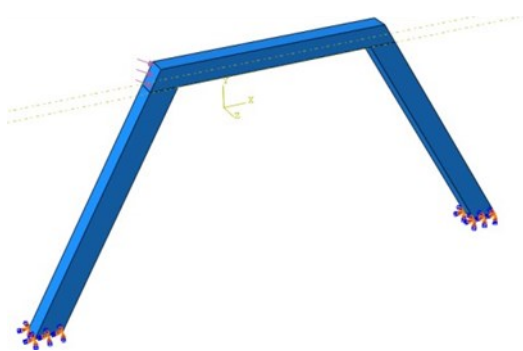


Figure 19. TBF

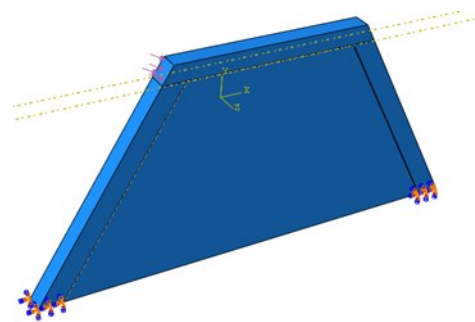


Figure 20. TIF

Boundary conditions were fixed at the bottom of the column. A horizontal lateral load of 10 kN was applied at the beam–column joint. Table 3 lists the characteristics of the materials used to model the trapezoidal RC bare frame and infilled frame.

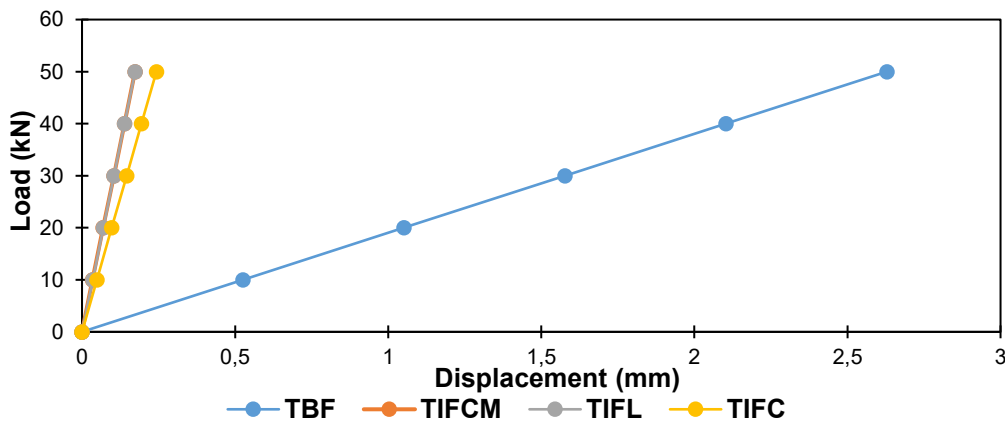


Figure 21. Load vs. storey displacement

Figures 19 and 20 depict the single-bay single-storey trapezoidal RC bare and infilled frames simulated using FEM-based software. The slope of the load versus displacement graph shown in Figure 21 is used to calculate the frame stiffness. The graph indicates that the stiffness of the TBF is 19 kN/mm under monotonic loading. The interface and infilled panels are discretised. Discretisation is an FE method used to break down a large piece into small parts [4]. Each division is independently investigated to acquire precise findings, and the cumulative behaviours of all parts are considered. The interface materials and infilled panels are modelled using a three-dimensional deformable solid extruded type element. In all cases, the thickness of the interface is assumed to be 10 mm. Four trapezoidal frame configurations with various interfaces are investigated. The frame designations are listed in Table 8.

**Table 8. Designation of trapezoidal frame configurations used**

Frame Designation	Description
<b>TBF</b>	Trapezoidal Bare Frames
<b>TIFCM</b>	Trapezoidal Infilled Frame with Cement Mortar Interface
<b>TIFL</b>	Trapezoidal Infilled Frame with Lead Interface
<b>TIFC</b>	Trapezoidal Infilled Frame with Cork

As listed in Table 9, the single-bay single-storey TIF has a rigidity of 289.03 kN/mm under monotonic loading. The TIFCM was initially modelled. Then, its interface was replaced by lead and cork; analyses were performed in the same manner. For the frame with lead and cork interfaces, the stiffness values were found to be 288,11 and 206,16 kN/mm, respectively. A comparative evaluation of stiffness for the single-bay single-storey frame with three different material interfaces is presented in Table 9. In a comparative study of different interface materials, specifically cement mortar, lead, and cork, the lateral stiffness of the infilled frame was found to be 15,19; 15,15; and 10,84 times the stiffness of the corresponding TBF, respectively; that is, the stiffness decreased with the modulus of elasticity of the interface material. Table 9 indicates that the TIFCM has the maximum stiffness.

**Table 9. Comparison of stiffness**

Type of Frame	Stiffness (kN/mm)
<b>TBF</b>	19,02
<b>TIFCM</b>	289,03
<b>TIFL</b>	288,11
<b>TIFC</b>	206,16

Compared with all frames, the TIF with traditional cement mortar as interface has the highest stiffness value. The stiffness is expected to increase when lead interface is used. However, the use of cork interface is anticipated to yield a lower stiffness value, and the frame is bound to exhibit bare-frame action. This investigation proceeded to the next phase by conducting experiments. In this phase, no of out-of-plane failure did not occur in the cement mortar or cork. Similarly, this failure did not occur in the rectangular frames with cement mortar or cork interfaces [22, 23].

#### **4.5 Effects of window openings with different sizes and positions on TIF under static loading**

The effects of various opening sizes and positions on the TIF and the seismic performance of RC infilled frames are discussed in this section. Under monotonic loading, the problem is investigated in an elastic area. In addition, the stiffness reduction ratio,  $\lambda$ , defined as the ratio of the stiffness obtained from a frame with opening to the stiffness obtained from a fully infilled frame (i.e., without opening), was calculated and compared with that of an RIF (as conducted in a previous study).

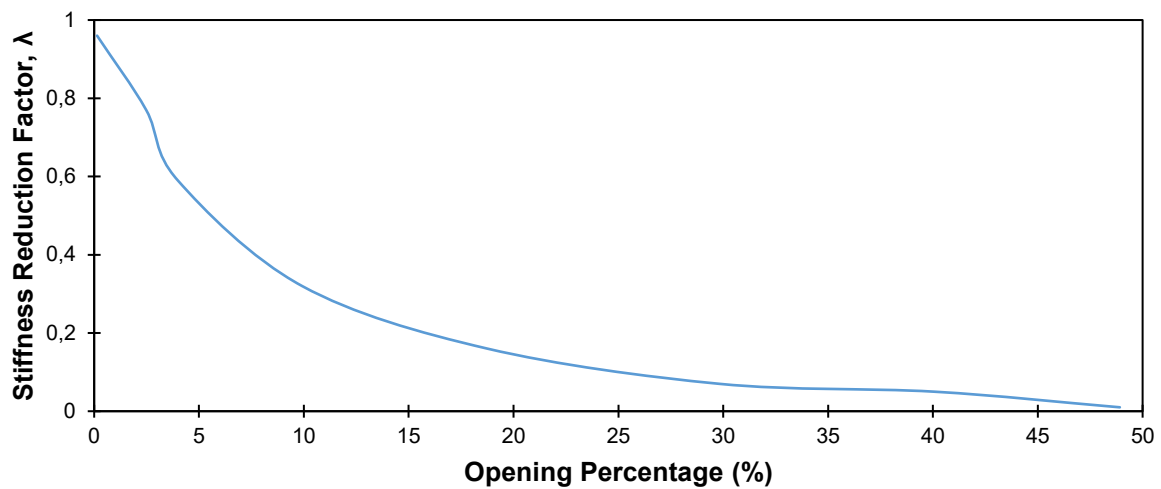


**Figure 22. Stiffness reduction factor,  $\lambda$ , of TIF in relation to opening percentage (Case C: opening on diagonal)**

The ABAQUS software package mentioned above was used to analyse a number of different single-bay single-storey trapezoidal infilled structures with various configurations. The structures were tested with a 10-kN horizontal load and a load distribution equivalent to that around the frame and infill brick panel. Table 3 lists the mechanical properties of both the RC frame and infilled brick masonry frame. The following parameters and instances were investigated to determine the effect of openings on the lateral stiffness or behaviour of infilled frames under static lateral loading:

1. Presence (or absence) of an opening in the infilled panel.
2. Percentage of opening = (Area of opening / Total infilled panel area).
3. Position of opening; the opening percentages of the following four cases were studied:
  - Case A: Opening on loading diagonal,
  - Case B: Opening at top centre,
  - Case C: Opening at centre between two diagonals,
  - Case D: Opening on off-loading diagonal.

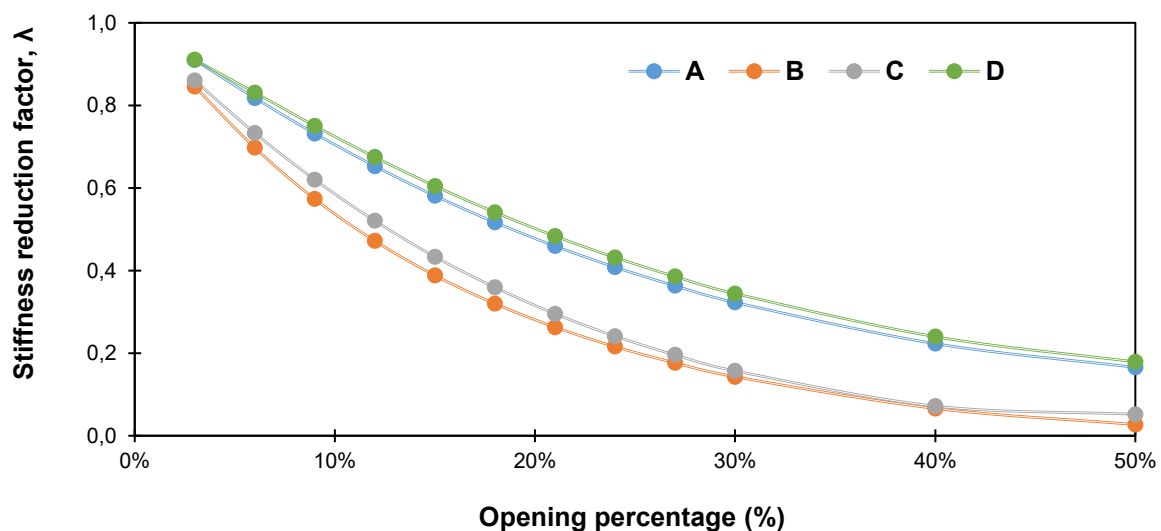


**Figure 23. Stiffness reduction factor,  $\lambda$ , of TIF in relation to opening percentage for different positions of openings**

#### 4.5.1 Stiffness Reduction Factor Calculation

As mentioned, the stiffness reduction factor is defined as the ratio of the stiffness obtained from a frame with opening to the stiffness of a fully infilled frame (without opening). This factor is given by Eq. (4), as follows:

$$\lambda = \frac{\Delta_x \text{Opening}}{\Delta_x \text{Full}} \quad (4)$$

The foregoing equation yields the lateral stiffness of the solid masonry infilled panel. Equations (5) and (6) yield the lateral stiffness of the infilled panel without ( $\Delta_x \text{ Full}$ ) and with opening ( $\Delta_x \text{ Opening}$ ), respectively:

$$\Delta_x \text{ Full} = \Delta_x F - \Delta_x B \quad (5)$$

$$\Delta_x \text{ Opening} = \Delta_x O - \Delta_x B \quad (6)$$

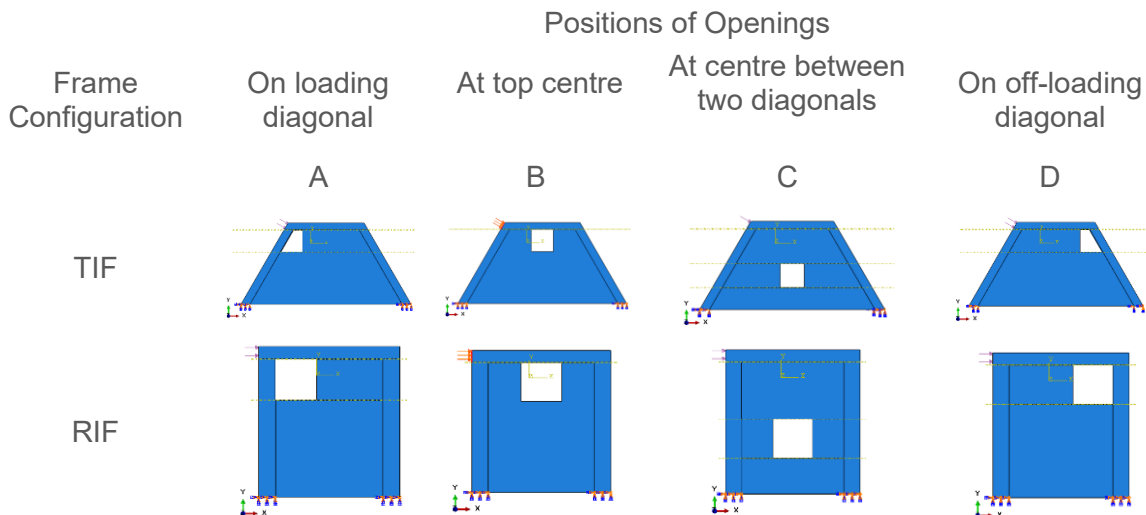
Where:

$\Delta_x F$  denotes stiffness of the fully infilled frame,

$\Delta_x B$  denotes stiffness of the bare frame,

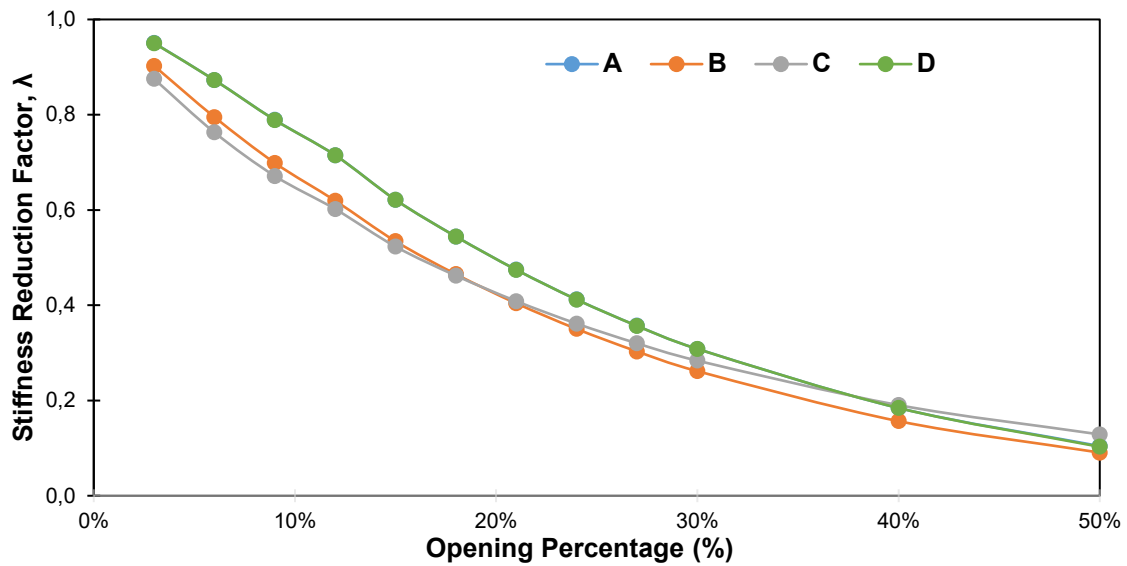
$\Delta_x O$  denotes stiffness of the infilled frame with opening.

Figure 22 shows Case A with an opening on the diagonal of the TIF. As expected, increasing the percentage of openings reduces the rigidity of the frame. A 51 % reduction in rigidity was observed compared with the rigidity of the bare frame. The stiffness factor remained virtually constant for openings greater than 50 %. Figure 23 shows the effects of openings on the stiffness of TIFs. The stiffness corresponding to the four positions of openings is reduced when the percentage of opening increases. The figure shows the behaviour of the stiffness reduction factor of TIFs as a function of opening percentage. When the opening was diagonal, the stiffness reduction factor appeared to be higher. The various positions of the opening region in the masonry infilled panel are illustrated in Figure 24.



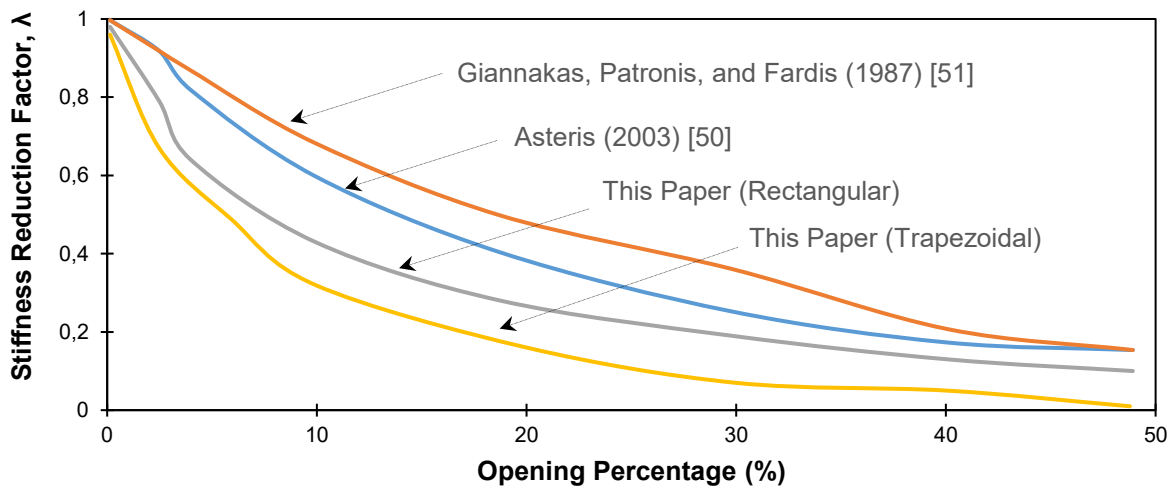
**Figure 24. Various positions of openings in masonry infilled panel**

Figure 25 shows the impact of the opening on the stiffness reduction of RIFs considering four different regions in the opening. The stiffness reduction factor appeared to be higher when the opening was diagonal. This is because the effect of the compressed diagonal on the infilled frame is negated in this case [50].



**Figure 25. Stiffness reduction factor,  $\lambda$ , of RIF in relation to opening percentage considering different opening positions**

The foregoing figure indicates that the opening at the centre between the diagonal has the least stiffness reduction factor. However, at a certain limit (Case C: opening on diagonal), the stiffness reduction value increases. The figure further indicates that frame rigidity decreases as the percentage of openings increases. Therefore, in all cases, such as A, B, and D, the stiffness decreases as the opening increases. In contrast, when the opening is on the diagonal, the stiffness is high at a certain percentage of opening owing to the arch action of the infilled panel.



**Figure 26. Stiffness reduction factor,  $\lambda$ , of infilled frame in relation to opening percentage (Case C: opening on diagonal)**

Figure 26 displays the validation results of the current analysis compared with the prior analytical results of [50] and [51] on the effects of the percentage of opening on the diagonal. In this scenario, the consistency between the current and previous analytical results is considerable.

#### 4.6 Effects of three different combinations of interfaces on intermediate stiffness of TIF

A paper cited in this study reports that the use of cork or lead at the interface renders the lateral stiffness of an infilled frame to be similar to that of a bare frame.

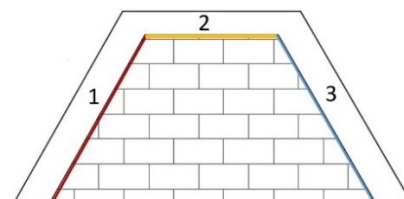
To identify the critical model for determining the higher and medium stiffness values obtained by modifying the interface properties, an analytical investigation was implemented.

**Table 10. TIF with different interface combinations**

Frame configuration	Details of interface in frame		
	1	2	3
F1	CM	CM	CM
F2	L	L	L
F3	C	C	C
F4	CM	CM	L
F5	CM	CM	C
F6	CM	L	CM
F7	CM	L	L
F8	CM	C	CM
F9	CM	C	C
F10	L	L	CM
F11	L	L	C
F12	L	CM	CM
F13	L	CM	L
F14	L	C	L
F15	L	C	C
F16	C	C	CM
F17	C	C	L
F18	C	CM	CM
F19	C	CM	C
F20	C	L	L
F21	C	L	C
F22	CM	L	C
F23	CM	C	L
F24	L	CM	C
F25	L	C	CM
F26	C	CM	L
F27	C	L	CM

Interface Description: CM, Cement Mortar; L, Lead; C, Cork

Positions (sides) of Interface



The properties of the frame and infill materials were maintained, but the interface properties were varied. Different cases were generated by combining three interface materials (cement mortar, lead, and cork). The changes in the interface media are summarised in Table 9. This illustrates the necessity for a parametric study to achieve the best interface pattern. The storey stiffness was studied by applying a 10-kN in-plane lateral symmetrical load. A total of 27 combinations were generated, and the corresponding lateral displacements were observed. The combination chart includes cases of all frames with the same interface materials (three cases, F1–F3). Next, 19 cases (F4–F21) are created with two material combinations. Six combinations (F22–F27) were formed by combining the three materials.

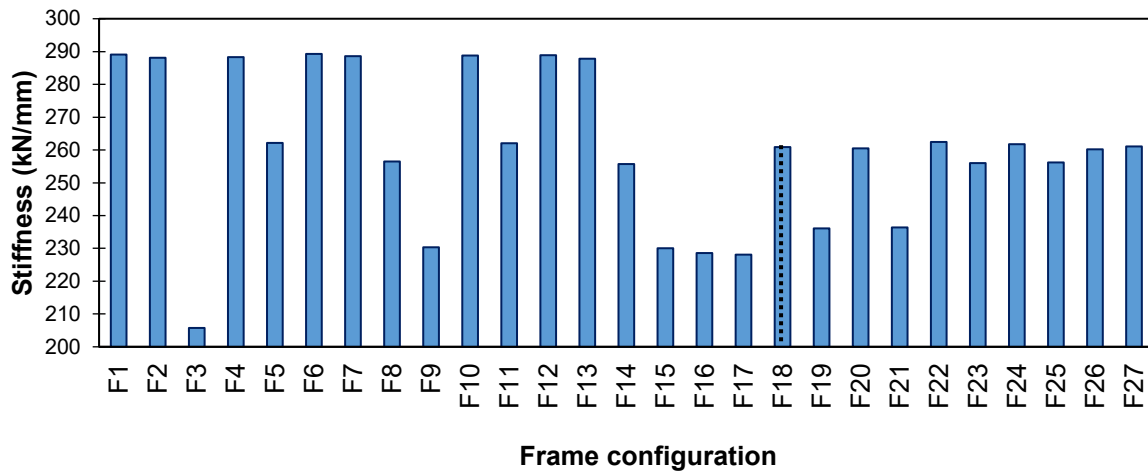


**Figure 27. Comparison of stiffness of TIFs with different configurations**

Simulations are implemented on F4-F21, which have two interface material combinations. The stiffness of some of these configurations was low. In some cases, it was high, even higher than that of F1. Simulations were also conducted on A22–A27, which consisted of three interface materials at different positions.

All the models were analysed by applying a lateral monotonic load of 10 kN. The stiffness of the frame with the F1 configuration (cement mortar interface material on all three sides of the TIF) was found to be the highest among the 27 configurations (i.e., 289,05 kN/mm). In contrast, a drop in stiffness (29 % less than that of the highest stiffness) was observed in the frame with the F3 configuration. The stiffness of the frame with the F2 configuration (lead interface) was found to decrease by only 0,3 %. The stiffness of the frame with the F18 configuration (Figure 27) was intermediate (i.e., 260,88 kN/mm). This stiffness was found to be 10 % less than that of the frame with the F1 configuration. The F18 configuration consisted of cement mortar and cork. Therefore, the combination of these materials as interface results in a frame with intermediate stiffness.

## 5 Conclusions

The present analytical investigation describes the behaviour of a TIF subjected to monotonic lateral loading. The influence of interface materials (cement mortar, lead, and cork and their combinations) and openings of various sizes and positions compared with those of conventional rectangular frames was analysed. The following conclusions are drawn from the FEA results:

1. A single-bay single-storey RC trapezoidal frame was modelled and analysed using the FE software ABAQUS. An optimum angle of 60° was used as the column inclination of the trapezoidal frame. This angle was found to yield the maximum stiffness compared with the other column inclinations. This leads to the conclusion that a trapezoidal frame with a 60° column inclination was optimal.

2. The single-bay single-storey RC trapezoidal frame configuration was analysed and compared with the rectangular frame configuration. The following were observed:
  - The trapezoidal frame structure appeared to be more rigid than the rectangular frame configuration. The stiffness values of the trapezoidal frame were 55 % and 60 % greater than those of the rectangular frame considering bare and infilled frames, respectively.
  - In the linear analysis, the moment of the bare frame was evidently higher than that of the infilled frame. However, the shear of the bare frame was lower than that of the infilled frame. This demonstrates that when an infill is introduced, the frame becomes less ductile than the bare frame. Consequently, material failure rather than structural failure occurs.
  - The trapezoidal frame has a higher lateral rigidity than the rectangular frame; consequently, its bending moment and shear force are found to be lower.
  - The trapezoidal structure can withstand greater lateral loads owing to the inclination of the column. The column inclination behaves as a strut in resisting lateral loads, thus consuming a considerable amount of energy.

The foregoing shows that the trapezoidal-type configuration can be utilised in high-rise structures and in areas with strong seismic forces because of its superior lateral load resistance, which can avert disaster.

3. A single-bay single-storey RC TBF and three infilled frames with different interface materials (cement mortar, cork, and lead) were modelled and analysed using the FEA software ABAQUS. A comparison of the analysis results considering four frames leads to the following conclusions:
  - The infilled frame has higher lateral rigidity than the bare frame.
  - The stiffness of TIFs with a cement mortar interface was higher than that of those with lead and cork interfaces.

Among all the frames studied, TIFs with the typical cement mortar interface have the maximum stiffness.

4. A detailed statistical investigation was performed on the effects of openings with various positions and sizes in a brick masonry panel on a trapezoidal frame. The frame was subjected to static lateral monotonic loading. In the analysis, the stiffness reduction factor was considered. The following conclusions are drawn:
  - The lateral stiffness of infilled frames decreased when the opening percentage increased. Compared with a bare frame, the reduction in lateral stiffness of infilled frames was 51 %. The stiffness factor remained virtually constant for openings greater than 50 %.
  - When the position of the opening moved diagonally (at the centre), the action between the frame and infill varied. When the opening was at the centre of the diagonal, the stiffness reduction factor appeared to be higher.
  - The trapezoidal frame configurations with various opening sizes and positions were compared with the rectangular frame configuration. In the case of the rectangular frame, positioning the opening on the diagonal increases the lateral stiffness to a certain percentage owing to the arch action failure of the infilled panel.

The analysis results lead to the conclusion that 50 % openings and openings on the diagonal are the critical size and position of openings, respectively.

5. The TIF was analysed considering different combinations of interfaces. The analysis results lead to the conclusion that the frame with the F1 configuration has the highest stiffness among the frames with 27 combinations. The F2 configuration yields the second highest stiffness, which is 0,3 % less than that of the highest

stiffness. The F3 configuration yields the least lateral stiffness. The frame with the F18 configuration (cement mortar and cork interface) has an intermediate stiffness among all the cases.

## References

- [1] Hamakareem, M. I. Types of High-Rise Buildings Structural Systems. The Constructor-Building ideas, Accessed: 21.03.2023. Available at: <https://theconstructor.org/structural-engg/high-rise-buildings-structural-systems/23076/>
- [2] Crisafulli, F. PPT-Analysis of Infill Frame Structures. SCRIBD, Accessed: 21.03.2023. Available at: <https://www.scribd.com/document/143760315/Crisafulli-F-J-PPT-Analysis-of-infill-frame-structures>
- [3] Allen, L.; Charleson, A.; Brzev, S.; Scawthorn, C. Reinforced concrete frame building with brick infill walls under construction. Taxonomy-Openquake, Accessed: 21.03.2023. Available at: <https://taxonomy.openquake.org/index.php/terms/infilled-frame>
- [4] Kumar, S. M.; Sarany, G.; Lakshmiathy, M.; Satyanarayanan, K. S. Modeling and Study of Behavior of Infilled Frames with Different Interface Materials under Static Loading. *Indian Journal of Science and Technology*, 2016, 9 (23), pp. 1-6. <https://doi.org/10.17485/ijst/2016/v9i23/95973>
- [5] Smith, B. S. Methods for predicting the lateral stiffness and strength of multi-storey infilled frames. *Building Science*, 1967, 2 (3), pp. 247-257. [https://doi.org/10.1016/0007-3628\(67\)90027-8](https://doi.org/10.1016/0007-3628(67)90027-8)
- [6] Pantò, B.; Silva, L.; Vasconcelos, G.; Lourenço, P. B. Macro-modelling approach for assessment of out-of-plane behavior of brick masonry infill walls. *Engineering Structures*, 2019, 181, pp. 529-549. <https://doi.org/10.1016/j.engstruct.2018.12.019>
- [7] Karayannis, Ch. G.; Kakaletsis, D. J.; Favvata, M. J. Behavior of bare and masonry infilled R/C frames under cyclic loading: Experiments and analysis. *WIT Transactions on The Built Environment*, 2005, 81, pp. 429-438.
- [8] Baker, J. W. Measuring bias in structural response caused by ground motion scaling. In: *8th Pacific Conference on Earthquake Engineering (8PCEE 07)*. 5-7<sup>th</sup> December 2007, Singapore; 2007.
- [9] Zhang, C. et al. Seismic performance of semi-rigid steel frame infilled with prefabricated damping wall panels. *Journal of Constructional Steel Research*, 2021, 184. <https://doi.org/10.1016/j.jcsr.2021.106797>
- [10] Nigel Priestley, M. J.; Michele Calvi, G. Towards a capacity-design assessment procedure for reinforced concrete frames. *Earthquake Spectra*, 1991, 7 (3), pp. 413-437. <https://doi.org/10.1193/1.1585635>
- [11] Mallick, D. V.; Severn, R. T. The behaviour of infilled frames under static loading. *Proceedings of the Institution of Civil Engineers*, 1967, 38 (4), pp. 639-656. <https://doi.org/10.1680/iicep.1967.8192>
- [12] Emami, S. M. M.; Mohammadi, M. Effect of frame connection rigidity on the behavior of infilled steel frames. *Earthquakes and Structures*, 2020, 19 (4), pp. 227-241. <https://doi.org/10.12989/eas.2020.19.4.227>
- [13] Di Trapani, F. et al. Traditional vs. sliding-joint masonry infilled frames: Seismic reliability and EAL. *Procedia Structural Integrity*, 2020, 26, pp. 383-392. <https://doi.org/10.1016/j.prostr.2020.06.049>
- [14] Jalaeefer, A.; Zargar, A. Effect of infill walls on behavior of reinforced concrete special moment frames under seismic sequences. *Structures*, 2020, 28, pp. 766-773. <https://doi.org/10.1016/j.istruc.2020.09.029>
- [15] Mohamed, H.; Romão, X. Analysis of the performance of strut models to simulate the seismic behaviour of masonry infills in partially infilled RC frames. *Engineering Structures*, 2020, 222. <https://doi.org/10.1016/j.engstruct.2020.111124>

- [16] Murty, C. V. R.; Jain, S. K. Beneficial Influence of Masonry Infill Walls on Seismic Performance of Rc Frame Buildings. In: *12th World Conference on Earthquake Engineering*. 30<sup>th</sup> January – 4<sup>th</sup> February 2000, Auckland, New Zealand, New Zealand Society for Earthquake Engineering; 2000.
- [17] Marinković, M.; Butenweg, C. Innovative decoupling system for the seismic protection of masonry infill walls in reinforced concrete frames. *Engineering Structures*, 2019, 197. <https://doi.org/10.1016/j.engstruct.2019.109435>
- [18] De Risi, M. T. et al. Experimental investigation on the influence of the aspect ratio on the in-plane/out-of- plane interaction for masonry infills in RC frames. *Engineering Structures*, 2019, 189, pp. 523-540. <https://doi.org/10.1016/j.engstruct.2019.03.111>
- [19] Alwashali, H.; Sen, D.; Jin, K.; Maeda, M. Experimental investigation of influences of several parameters on seismic capacity of masonry infilled reinforced concrete frame. *Engineering Structures*, 2019, 189, pp. 11-24. <https://doi.org/10.1016/j.engstruct.2019.03.020>
- [20] Mohammadi, M.; Mirzaei, M.; Pashaie, M. R. Seismic performance and fragility analysis of infilled steel frame structures using a new multi-strut model. *Structures*, 2021, 34, pp. 1403-1415. <https://doi.org/10.1016/j.istruc.2021.08.015>
- [21] Smith, B. S.; Coull, A. *Tall Building Structures: Analysis and Design*. New York, USA: John Wiley / Sons, Inc. 1991.
- [22] Kumar, S. M.; Satyanarayanan, K. S. Study the effect of elastic materials as interface medium used in infilled frames. *Materialstoday: Proceedings*, 2018, 5 (2), pp. 8986-8995. <https://doi.org/10.1016/j.matpr.2017.12.343>
- [23] Satyanarayanan, K. S. *Studies on the influences of different interface materials on the elastic behavior of infilled frames*. [Doctoral thesis], SRM University, Chennai, India, 2009.
- [24] Sijata, J. et al. Conceptual paper on factors affecting the attitude of senior citizens towards purchase of smartphones. *Indian Journal of Science and Technology*, 2015, 8 (S4), pp. 83-89. <https://doi.org/10.17485/ijst/2015/v8iS4/62318>
- [25] Surendran, S.; Kaushik, H. B. Masonry Infill RC Frames with Openings: Review of In-plane Lateral Load Behaviour and Modeling Approaches. *The Open Construction and Building Technology Journal*, 2012, 6 (Suppl 1-M9), pp. 126-154. <http://dx.doi.org/10.2174/1874836801206010126>
- [26] Muthukumar, S.; Satyanarayanan, K. S.; Senthil, K. Studies on two bay and three storey infilled frame with different interface materials: Experimental and finite element studies. *Structural Engineering and Mechanics*, 2017, 64 (5).
- [27] Senthil, K.; Muthukumar, S.; Rupali, S.; Satyanarayanan, K. S. Effect of Various Interface Thicknesses on the Behaviour of Infilled frame Subjected to Lateral Load. In: *International Conference on Recent Advances in Materials, Mechanical and Civil Engineering*. 1-2<sup>nd</sup> June 2017, Hyderabad, India, IOP Conference Series: Materials Science and Engineering; 2018, 330. <https://doi.org/10.1088/1757-899X/330/1/012113>
- [28] Thirumurugan, V. et al. Behavior of Infilled Frames with Different Interface Materials. In: *National conference on Recent advancement and sustainability in Civil Engineering (RASCE 2015)*. 2015. Accessed: 22.03.2023. Available at: [https://www.researchgate.net/publication/316990250\\_Behavior\\_of\\_Infilled\\_Frames\\_with\\_Different\\_Interface\\_Materials](https://www.researchgate.net/publication/316990250_Behavior_of_Infilled_Frames_with_Different_Interface_Materials)
- [29] Umar, Z. et al. Innovative seismic isolation of masonry infills using cellular material at the interface with the surrounding RC frame. *Journal of Building Engineering*, 2021, 40. <https://doi.org/10.1016/j.jobbe.2021.102736>
- [30] Furtado, A.; Arêde, A.; Rodrigues, H.; Varum, H. The role of the openings in the out-of-plane behaviour of masonry infill walls. *Engineering Structures*, 2021, 244. <https://doi.org/10.1016/j.engstruct.2021.112793>
- [31] Penava, D.; Sarhosis, V.; Kožar, I.; Guljaš, I. Contribution of RC columns and masonry wall to the shear resistance of masonry infilled RC frames containing different in size

- window and door openings. *Engineering Structures*, 2018, 172, pp. 105-130. <https://doi.org/10.1016/j.engstruct.2018.06.007>
- [32] Sukrawa, M.; Budiwati, I. A. M. Analysis and design methods for infilled frames with confined openings. *International Journal of Technology*, 2019, 10 (2), pp. 394-404. <https://doi.org/10.14716/ijtech.v10i2.2467>
- [33] Anić, F. et al. Out-of-plane cyclic response of masonry infilled RC frames: An experimental study. *Engineering Structures*, 2021, 238. <https://doi.org/10.1016/j.engstruct.2021.112258>
- [34] Yekrangnia, M.; Asteris, P. G. Multi-strut macro-model for masonry infilled frames with openings. *Journal of Building Engineering*, 2020, 32. <https://doi.org/10.1016/j.jobbe.2020.101683>
- [35] Malick, D. V.; Garg, R. P. Effect of openings on the lateral stiffness of infilled frames. *Proceedings of the Institution of Civil Engineers*, 1971, 49 (2), pp. 193-209. <https://doi.org/10.1680/iicep.1971.6263>
- [36] Dias-Oliveira, J.; Rodrigues, H.; Asteris, P. G.; Varum, H. On the Seismic Behavior of Masonry Infilled Frame Structures. *Buildings*, 2022, 12 (8). <https://doi.org/10.3390/buildings12081146>
- [37] Cavaleri, L.; Zizzo, M.; Asteris, P. G. Residual out-of-plane capacity of infills damaged by in-plane cyclic loads. *Engineering Structures*, 2020, 209. <https://doi.org/10.1016/j.engstruct.2019.109957>
- [38] Lemonis, M. E.; Asteris, P. G.; Zitouniatis, D. G.; Ntasis, G. D. Modeling of the lateral stiffness of masonry infilled steel moment-resisting frames. *Structural Engineering and Mechanics*, 2019, 70 (4), pp. 421-429. <https://doi.org/10.12989/sem.2019.70.4.421>
- [39] Cavaleri, L.; Di Trapani, F.; Asteris, P. G.; Sarhosis, V. Influence of column shear failure on pushover based assessment of masonry infilled reinforced concrete framed structures: A case study. *Soil Dynamics and Earthquake Engineering*, 2017, 100, pp. 98-112. <https://doi.org/10.1016/j.soildyn.2017.05.032>
- [40] Asteris, P. G. et al. Parameters affecting the fundamental period of infilled RC frame structures. *Earthquakes and Structure*, 2015, 9 (5), pp. 999-1028. <http://dx.doi.org/10.12989/eas.2015.9.5.999>
- [41] Asteris, P. G. et al. On the fundamental period of infilled RC frame buildings. *Structural Engineering and Mechanics*, 2015, 54 (6), pp. 1175-1200. <http://dx.doi.org/10.12989/sem.2015.54.6.1175>
- [42] The Owner Builder Network. Daiko. Accessed: 22.03.2023. Available at: <https://theownerbuildernetwork.co/daiko/>
- [43] Mitra, S. Top 10 Japanese architecture trends of 2022. Yanko Design, Accessed: 22.03.2023. Available at: <https://www.yankodesign.com/2022/02/10/top-10-japanese-architecture-trends-of-2022/>
- [44] Banon, J. A. Garden House. Arch Daily, Accessed: 22.03.2023. Available at: <https://www.archdaily.com/306750/garden-house-joaquin-alvado-banon>
- [45] Kwiecień, A. et al. Use of polymer flexible joint between RC frames and masonry infills for improved seismic performance. In: *Proceedings of SMAR 2017, Fourth Conference on Smart Monitoring, Assessment and Rehabilitation of Civil Structures*. 13-15<sup>th</sup> September 2017, Zurich, Switzerland, 2017.
- [46] Riddington, J. R.; Sahota, M. K. Stability of lead alloy compressive work hardening. *Materials & Design*, 1999, 20 (1), pp. 13-17. [https://doi.org/10.1016/S0261-3069\(98\)00044-2](https://doi.org/10.1016/S0261-3069(98)00044-2)
- [47] Silva, S. P. et al. Cork: Properties, capabilities and applications. *International Materials Reviews*, 2005, 50 (6), pp. 345-365. <https://doi.org/10.1179/174328005X41168>
- [48] Kubalski, T.; Marinković, M.; Butenweg, C. Numerical investigation of masonry infilled R.C. frames. In: *Proceedings of the 16th International Brick and Block Masonry Conference*, Modena, C.; da Porto, F.; Valluzzi, M. R. (eds.). 26-30<sup>th</sup> June 2016, Padova, Italy, CRC Press; 2016. Pp. 1219-1226.

- [49] Muthu Kumar, S.; Joson Western, J.; Satyanarayanan, K. S. Nonlinear analysis of stresses for two bay three storeyed reinforced concrete infill frame. *International Journal of Chemical Sciences*, 2016 14 (S1), pp. 79-87.
- [50] Asteris, P. G. Lateral Stiffness of Brick Masonry Infilled Plane Frames. *Journal of Structural Engineering*, 2003, 129 (8), pp. 1071-1079.  
[https://doi.org/10.1061/\(ASCE\)0733-9445\(2003\)129:8\(1071\)](https://doi.org/10.1061/(ASCE)0733-9445(2003)129:8(1071))
- [51] Giannakas, A.; Patronis, D.; Fardis, M. The influence of the position and the size of openings to the elastic rigidity of infill walls. In: *Proceedings of the 8th Hellenic Concrete Conference*, pp. 49-56, 1987.
- [52] Bureau of Indian Standards. IS 456 (2000): Plain and Reinforced Concrete – Code of Practice. Accessed: 22.03.2023. Available at: <https://www.iitk.ac.in/ce/test/IS-codes/is.456.2000.pdf>